Possible Phase Transition Deep Inside the Hidden Order Phase of Ultraclean URu$_2$Si$_2$

H. Shishido[1], K. Hashimoto[1], T. Shibauchi[1], T. Sasaki[2], H. Oizumi[2], N. Kobayashi[2], T. Takamasu[3],

K. Takehana[3], Y. Imanaka[3], T. D. Matsuda[4], Y. Haga[4], Y. Onuki[4,5], and Y. Matsuda[1]

[1]*Department of Physics, Kyoto University, Kyoto 606-8502, Japan*
[2]*2Institute for Materials Research, Tohoku University, Sendai 980-8577, Japan*
[3]*National Institute for material Science, Tsukuba, Ibaraki 305-0047, Japan*
[4]*Advanced Science Research Center, Japan Atomic Energy Agency, Tokai 319-1195, Ibaraki, Japan and*
[5]*Graduate School of Science, Osaka University, Toyonaka, Osaka 560-0043, Japan*

To elucidate the underlying nature of the hidden order (HO) state in heavy-fermion compound URu$_2$Si$_2$, we measure electrical transport properties of ultraclean crystals in a high field/low temperature regime. Unlike previous studies, the present system with much less impurity scattering resolves a distinct anomaly of the Hall resistivity at H^*=22.5 T well below the destruction field of the HO phase $\simeq$36 T. In addition, a novel quantum oscillation appears above a magnetic field slightly below H^*. These results indicate an abrupt reconstruction of the Fermi surface, which implies a possible phase transition well within the HO phase caused by a band-dependent destruction of the HO parameter. The present results definitely indicate that the HO transition should be described by an itinerant electron picture.

The heavy fermion compound URu$_2$Si$_2$ has held attention of physicists for the past two decades owing to the presence of a 'hidden order' (HO) transition at T_c=17.5 K [1, 2, 3]. Tiny magnetic moment appears ($M_0 \sim 0.02\mu_B$) below T_c [4], but M_0 is by far too small to explain the large entropy released during the transition. Several exotic order parameters have been proposed for the HO phase[5], which are based on either itinerant or localized pictures. However, the genuine HO parameter is still an open question. Its elucidation is very important as it can lead to a discovery of new order parameters in strongly correlated electron systems.

Several remarkable features of the HO phase have been reported experimentally. The electronic excitation gap is formed at a large portion of the Fermi surface (FS) below T_c and most of the carriers ($\sim$90%) disappears, resulting in a semimetallic state [6, 7, 8, 9]. The remaining small number of carriers undergo a transition into an exotic superconducting state at T_{sc}=1.45 K [9, 10, 11]. The neutron scattering experiments report the appearance of commensurate and incommensurate inelastic magnetic responses in the HO phase [4, 12, 13]. The HO is affected by external parameters, such as pressure and magnetic field. Above the critical pressure of $\sim$0.5 GPa, a true antiferromagnetic ordered state with large moments ($\sim$ 0.4μ_B/U) emerges [14, 15], but no dramatic modification of the Fermi surface is reported between the HO and antiferromagnetic phases [16, 17, 18, 19]. In contrast, strong magnetic fields destroy the HO phase accompanying a radical reconstruction of the FS [20, 21, 22, 23, 24, 25]. Well below T_c, field-induced destruction of the HO occurs at $H_c \simeq$36 T.

Thus high magnetic field response is a clue for elucidating the HO parameter. To date high field studies have been carried out by using crystals with rather low residual resistivity ratio (RRR). Recently, extremely large magnetoresistance has been reported in the crystals with a very large $RRR(\sim 700)$ [9, 10]. Such ultraclean crystals are expected to develop an advanced understanding about the HO phase. Here we present the Hall effect, magnetoresistance and quantum oscillation measurements in the HO state of the ultraclean crystals. We find several salient features which have never been reported in crystals with lower RRR values, including a band-dependent destruction of the HO parameter and a possible transition deep inside the HO phase.

The URu$_2$Si$_2$ single crystals were grown by the Czochralski pulling method in a tetra-arc furnace [26]. The crystal used in this study displays a very low in-plane residual resistivity $\rho_0 \simeq 0.47$ $\mu\Omega$ cm and RRR is 670 [9]. The Hall effect and magnetoresistance were measured simultaneously up to 27 T in a transverse geometry for $\boldsymbol{J} \| a$ and for $\boldsymbol{H}$ within the bc-plane. Figure 1(a) displays the field dependence of the diagonal resistivity ρ_{xx} well below T_c. The magnetoresistance $\Delta\rho_{xx}(H)/\rho_{xx}(0) \equiv \frac{\rho_{xx}(H)-\rho_{xx}(0)}{\rho_{xx}(0)}$ is extremely large, $\sim$1200 at 25 T and T=0.11 K. Here we obtained $\rho_{xx}(0)$ by the extrapolation of the normal state resisitivity in zero field above T_{sc}, assuming $\rho_{xx}(T) = \rho_0 + AT^2$. At very low temperatures, the Shubnikov-de Haas (SdH) oscillations are clearly seen. As shown in the inset of Fig. 1(a), ρ_{xx} exhibits nearly H^2-dependence in the low field regime. No saturating behavior is observed for any field directions. Such an exceptionally large magnetoresistance arises from the combination of the peculiar electronic structure, i.e. extremely high purity, very low carrier density, and nearly perfect compensation (equal number of electrons and holes) [9, 27].

The field dependence of the Hall resistivity ρ_{xy} is displayed in Fig. 1(b). The quantum oscillations are also seen clearly. There are two characteristic fields marked by H_p (blue dashed arrows) and H^* (black solid arrows). With increasing H, ρ_{xy} increases almost linearly and decreases after showing a maximum at H_p. This
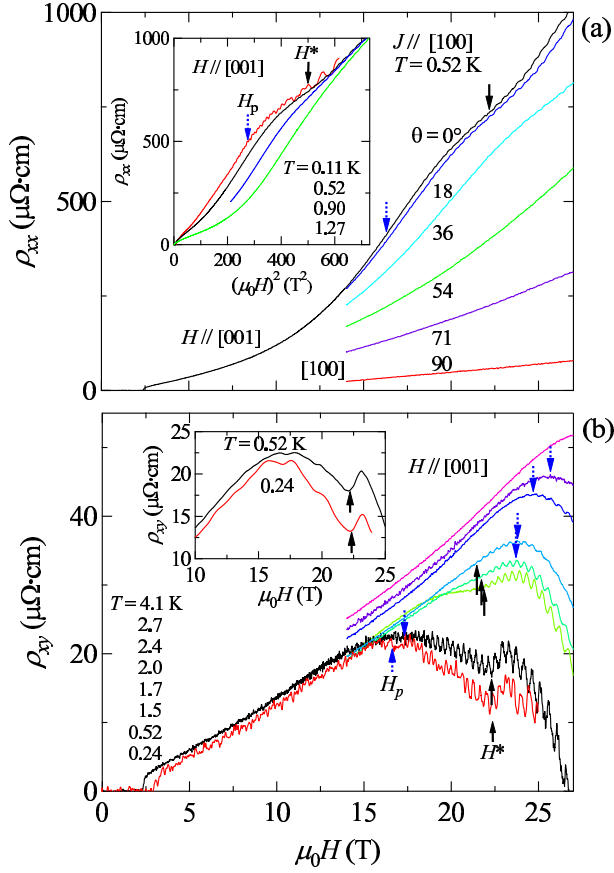
FIG. 1: (color online) (a) H-dependence of ρ_{xx} well below the HO transition for several field orientations. θ is the angle between $\boldsymbol{H}$ and the c-axis. Inset: ρ_{xx} plotted as a function of H^2. (b) H-dependence of ρ_{xy} at several temperatures for $\boldsymbol{H} \parallel c$. The oscillation in ρ_{xy} mainly arises from the ε band. Inset: Field dependence of ρ_{xy} in which the oscillatory part is removed. In each figure, the peak field H_p and H^* are marked by the blue dashed and black solid arrows, respectively.

FIG. 2: (color online)(a)FFT of the SdH oscillations in the field range 17-24 T for $\boldsymbol{H} \parallel c$ at T=0.11 K. Inset: Angular variation of the SdH frequency for each branch. (b) The power spectrum of the SdH oscillations (inverse of the frequency vs. $1/H$) displayed by the method of the continuous wavelet transform. (c) FFT of the SdH oscillations in the several field interval. Newly appeared ε-branch is shown by the hatched region.

broad peak of ρ_{xy} is consistent with previous reports [24]. At T=0.52 K and 0.24 K, ρ_{xy} exhibits another distinct anomaly at H^*=22.5 T. This anomaly is less pronounced at elevated temperatures. To see this more clearly, the inset of Fig. 1(b) displays $\rho_{xy}(H)$, in which the oscillatory part is removed. At H^*, ρ_{xy} exhibits a jump in a very narrow field range ($\Delta H \lesssim 1$ T). We stress that this distinct anomaly of ρ_{xy} at H^* is a characteristic feature of the ultraclean crystals, not reported previously. These anomalies can also be seen in ρ_{xx}. As shown in the inset of Fig. 1(a), ρ_{xx} deviates from H^2-dependence above $\simeq H_p$ and changes its slope again at H^*.

Before analyzing the data, we briefly discuss the electronic structure in the low field regime of the HO phase. Previous de Haas-van Alphen effect studies in fields up to 17 T resolved three frequencies for α-, β- and γ- FS sheets, which correspond to F_α=1.05 kT, F_β=0.42 kT and F_γ=0.19 kT with effective masses m_α=13m_0, m_β=25m_0, and m_γ=8.2m_0, respectively, where m_0 is the free electron mass [17, 28, 29]. Here,
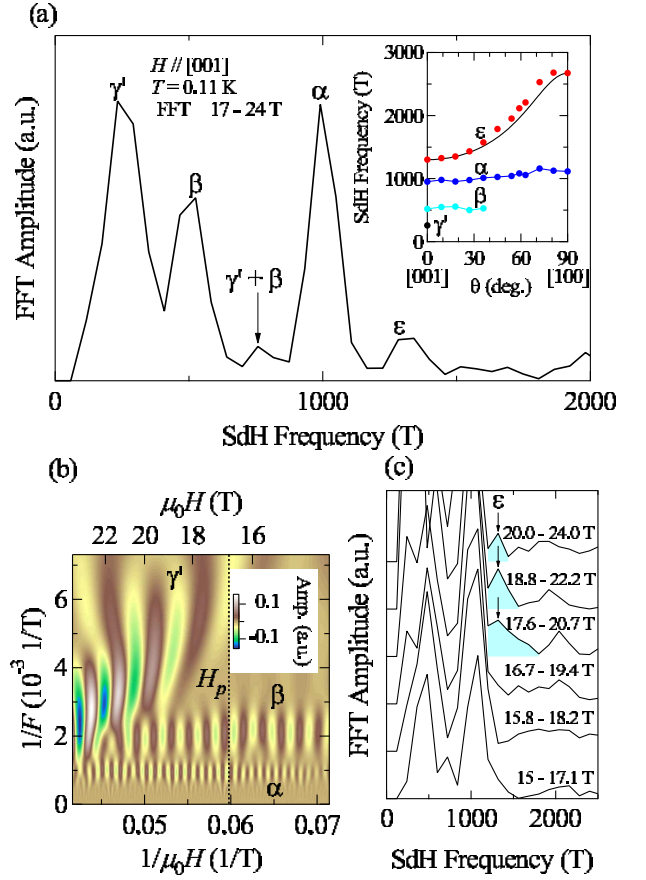
F_i is proportional to the cross-sectional area S_i of the i-th FS, $F_i = \hbar S_i/2\pi e$. It has been shown that the largest α-band is spherical and its volume corresponds to nearly 0.03 carriers per U-atom. This value is close to the carrier number extracted from the Hall coefficient, indicating that the α-band is a hole FS ($\rho_{xy} > 0$) and governs the transport properties. However the large Sommerfeld constant in the heat capacity(~ 80 mJ/K^{2}mol) [2] can not be accounted for the light α-FS sheet, indicating the presence of missing heavy electron band [9].

We now move on to the transport properties in the high field regime of the HO phase. Figure 2(a) displays the fast Fourier transform (FFT) of the SdH oscillations observed in ρ_{xx} for the field range between 17 and 24 T at $T = 0.11$ K. The branches which correspond to the α- and β-FS sheets are observed. The effective masses and the angular variation of the frequencies (inset of Fig. 2(a)) of these branches are very close to those reported in the low field regime [17, 28, 29]. A peak whose frequency is

close to the γ-FS sheet in the low field regime, which is assigned as γ', is also observed. However the obtained effective mass $m_{\gamma'} = 27\ m_0$ is much larger than the low field value. Another branch of the SdH oscillations, δ-branch with F_δ=0.59 kT, has been reported in Ref.[23] above 25 T. However, this branch is not observed in the present crystals. To examine the detailed field dependence of the frequency and amplitude of the SdH oscillations, we display in Fig. 2(b) the power spectrum of the oscillations yielded by means of the continuous wavelet transform. It is notable that the γ'-branch emerges above H_p and its frequency exhibits a large shift with H.

Another remarkable feature is the appearance of a new quantum oscillation, which is assigned as ε-FS sheet in Fig. 2(a). As shown in the inset of Fig. 2(a), this ε-sheet is elliptical and its volume is nearly three times larger than the volume of the α-sheet. The effective mass of the ε-sheet is $m_\varepsilon = 2.7m_0$, which is less than 30% of m_α. Figure 2(c) displays the FFT spectrum obtained in the various field ranges. While the ε-branch is not observable in the field range 16.7-19.4 T, it emerges in the range above 17.6-20.7 T (hatched area). Generally, quantum oscillations arising from heavier bands decay faster with decreasing H. Therefore, the fact that other branches with heavier masses are clearly observed in the whole H-range indicates that the low-field disappearance of the ε-branch with very light mass is not due to the decrease of the amplitude caused by the decrease of H.

Next we discuss the peculiar H-dependence of ρ_{xy} characterized by H_p and H^*. A plausible explanation for the decrease of ρ_{xy} above H_p, together with the concomitant deviation from the H^2-dependence of ρ_{xx}, is a violation of the nearly perfect compensation realized in the low field regime. This is supported by the continuous evolution of the FS across H_p, as evidenced by the development of γ'-FS sheet below H_p shown in Fig. 2(b). Such a FS evolution may come from the polarization of γ'-FS sheet, i.e. the shrinkage of one of the spin-split sheets to a point which occurs when the large Zeeman energy exceeds the Fermi energy [30]. In fact, the γ'-band with a small volume and a large effective mass should have a small Fermi energy.

The transport anomaly at H^* provides several pieces of important information for the electronic structure in the HO state. We point out that the anomaly at H^* is likely to be related to the appearance of the ε-FS sheet because of the following reason. Figure 3(a) depicts the angular variations of H^* (solid squares) and the amplitude of SdH oscillations of the ε-FS sheet (solid circles) in the field range of 20 - 27 T. H^* increases steeply with increasing θ. The solid line is the SdH amplitude calculated from the Lifshitz and Kosevich formula [31]. The observed SdH amplitude decreases faster than the value expected in the Lifshitz and Kosevich formula at $\theta \gtrsim 40°$, where H^* is out of the measurement range. We note that at $\theta \gtrsim 40°$ the ε-branch recovers in a higher field range of 24 - 27 T, indicating that the reduction in the field range of 20 -27 T is not due to the spin factor. There-
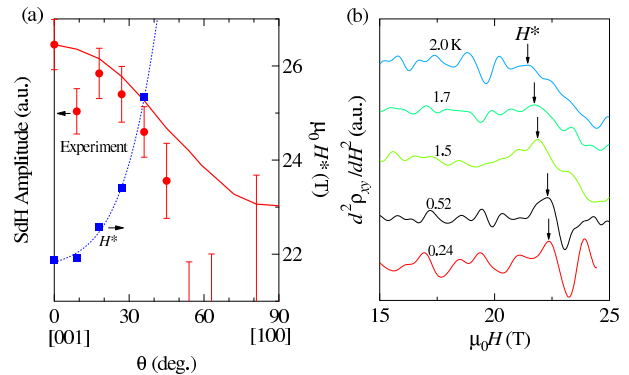

FIG. 3: (color online) (a) Solid (blue) squares indicate the angular variation of H^* determined by the inflection point of $\rho_{xx}(H)$, which is obtained by the field derivative of ρ_{xx}. Dashed line is a guide for the eye. Solid (red) circles indicate the angular dependence of SdH amplitude at T=0.52 K. The solid line is the result of the Lifshitz and Kosevich formula. (b) Field dependence of the second derivative of ρ_{xy} with respect to H. The oscillatory part in ρ_{xy} is filtered. The arrows indicate H^*.

fore, the depression of the ε-branch in the field range of 20 -27 T indicates the correlation between H^* and the SdH oscillation of the ε-branch. The quantum oscillation of the ε-branch starts at fields slightly below H^*. Such a precursor phenomenon is often observed in magnetic systems and in superconductors. As seen in Fig. 1(b), $\rho_{xy}(H)$ decreases more rapidly above H^* than below H^* and appears to become negative above 27 T at T=0.52 K. Such a sign change indicates that the ε-FS is an electron pocket with high mobility.

It has been reported that new quantum oscillations often appear when the metamagnetic transition or magnetic breakdown occurs. However, in either case, the jump of ρ_{xy} has never been observed [30, 32]. Therefore it is natural to attribute the observed twofold anomalies, namely the jump of ρ_{xy} and the appearence of the ε-FS sheet, to an abrupt reconstruction of the FS, which is caused by a possible phase transition at H^*. Since the electronic specific heat of the ε-band estimated from the SdH results is only $\gamma_\varepsilon \simeq 2.3$ mJ/K^2 mol, which is much less than the Sommerfeld constant, very accurate thermodynamic measurements are required to detect this transition.

We emphasize that the Hall sign change as well as the jump of ρ_{xy} is observed in the ultraclean crystals for the first time. Therefore it is very likely that these anomalies originate from the band-dependent nature of the HO parameter, because each band manifests their characters when the interband scattering is strongly suppressed with high purity. In such a case, each band has a different amplitude of the HO gap. Then new bands can appear when the magnetic field exceeds the condensation energy of the smaller HO gap even well below H_c, at which the complete destruction of the HO state occurs. This appearance of new bands would greatly change the properties of
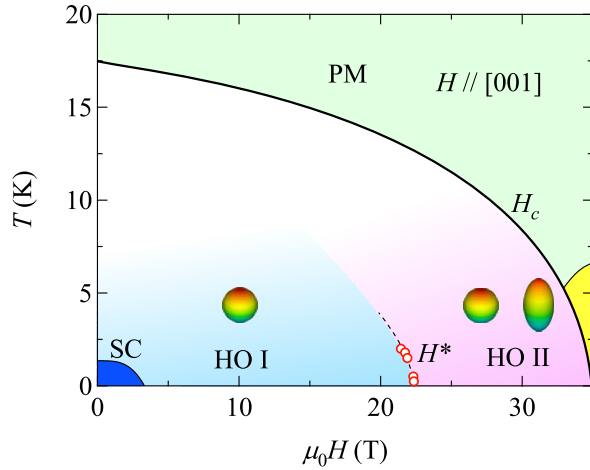
FIG. 4: (color online) $H - T$ phase diagram for $\boldsymbol{H} \| c$. SC and PM denote superconducting and paramagnetic regions respectively. The thick solid line is the critical field H_c of the hidden order (HO) state [20, 21, 23, 24, 25]. The red circles are H^* (see Fig. 3(b)), separating two distinguished HO state, HO I and HO II. Spherical band sketches the (hole) α-FS sheet. HO II is characterized by the appearence of the elliptical (electron) ε-FS sheet. The high field region above H_c shown by yellow is the field induced phase [20, 23, 24].

the electron orbits. This situation bears striking resemblance to the multiband superconductors such as MgB_2, in which the amplitude of the superconducting order parameter is band dependent. In this case, the superconductivity with the smaller gap is strongly suppressed at a "virtual upper critical field" well below the true upper critical field [9, 33]. Note that the multiband superconducting nature is observable only in clean systems where the interband mixing is weak.

Finally we discuss the $H - T$ phase diagram. The temperature dependence of H^* is determined by the kink positions in $d^2\rho_{xx}/dH^2$ vs. H curves, shown in Fig. 3(b). As the temperature is increased, H^* decreases gradually. Figure 4 displays the phase diagram obtained by the present study. The results strongly suggest that the HO phase contains two distinguished phases, HO I and HO II, each having different FS in the reciprocal space (see sketches in Fig. 4).

In summary, the transport studies by using ultraclean crystals of URu_2Si_2 reveal several outstanding features in the hidden order phase. Particularly, the observed transport anomalies and the appearance of a new quantum oscillation indicate an abrupt reconstruction of the Fermi surface. This implies a possible phase transition well within the HO phase caused by a band-dependent destruction of the hidden order parameter. Our finding places a constraint on theories of the hidden order state, which has been discussed by localized or itinerant electron picture. The band-dependent nature definitely indicates that the hidden order transition should be described by an itinerant picture.

[1] T. T. M. Palstra *et al.*, Phys. Rev. Lett. **55** 2727 (1985).
[2] M. B. Maple *et al.*, Phys. Rev. Lett. **56**, 185 (1986).
[3] W. Schlabitz *et al.*, Z. Phys. B **62**, 171 (1986).
[4] C. Broholm *et al.*, Phys. Rev. B. **43**, 12809 (1991).
[5] N. Shah, *et al.*, Phys. Rev. B **61**, 564 (2000). P. Santini and G. Amoretti, Phys. Rev. Lett. **73**, 1027 (1994). A. E. Sikkema *et al.*, Phys. Rev. B **54**, 9322 (1996). C.M. Varma and L. Zhu, Phys. Rev. Lett. **96**, 036405 (2006). V.P. Mineev and M.E. Zhitomirsky, Phys. Rev. B **72**, 014432 (2005). P. Chandra, *et al.* Nature (London) **417**, 831 (2002).
[6] J. Schoenes, *et al.*, Phys. Rev. B **35**, 5375 (1987).
[7] R. Bel *et al.*, Phys. Rev. B **70**, 220501(R) (2004).
[8] K. Behnia *et al.*, Phys. Rev. Lett. **94**, 156405 (2005).
[9] Y. Kasahara *et al.*, Phys. Rev. Lett. **99**, 116402 (2007).
[10] R. Okazaki *et al.*, Phys. Rev. Lett. **100**, 037004 (2008).
[11] K. Yano *et al.* Phys. Rev. Lett. **100**, 017004 (2008).
[12] R. Wiebe *et al.* Nature Phys. **3**, 96 (2007).
[13] A. Villaume *et al.*, Phys. Rev. B **78**, 012504 (2008).
[14] S. Uemura *et al.*, J. Phys. Soc. Jpn. **74**, 2667 (2005),
[15] H. Amitsuka *et al.* J. Magn. Magn. Mater. **310**, 214 (2007).
[16] E. Hassinger *et al.*, Phys. Rev. B **77**, 115117 (2008).
[17] M. Nakashima *et al.*, J.Phys. Condens. Matter **15**, S2011 (2003).
[18] J.R. Jeffries *et al.*, Phys. Rev. Lett. **99**, 217207 (2007).
[19] S. Elgazzar *et al.*, Nature Mater. DOI:10.1038/NMAT2395 (2009).
[20] M. Jaime *et al.*, Phys. Rev. Lett. **89**, 287201 (2002).
[21] J.S. Kim, D. Hall, P. Kumar, and G.R. Stewart, Phys. Rev. B **67**, 014404 (2003).
[22] J. Levallois *et al.* a preprint.
[23] Y.J. Jo *et al.*, Phys. Rev. Lett. **98**, 166404 (2007).
[24] Y.S. Oh *et al.*, Phys. Rev. Lett. **98**, 016401 (2007).
[25] N. Harrison, M. Jaime, and J.A. Mydosh, Phys. Rev. Lett. **90**, 096402 (2003).
[26] The site occupancy and chemical composition of the crystals were consistent with $ThCr_2Si_2$ stoichiometry within an experimental accuracy of <1 %
[27] A. B. Pippard, *Magnetoresistance in metals*, (Cambridge Univ. Press, Cambridge, 1989).
[28] H. Ohkuni *et al.*, Philo. Mag. B **79**, 1045 (1999).
[29] C. Bergemann *et al.*, Physica B **230-232**, 348 (1997).
[30] R. Daou, C. Bergemann, and S.R. Julian, Phys. Rev. Lett. **96**, 026401 (2006).
[31] I.M. Lifshitz and A.M. Kosevich, Zh. Eksp. Teor. Fiz., **29**, 730 (1955) (Sov. Phys. JETP, **2**, 636 (1956)).
[32] M. M. Honold *et al.*, Phys. Rev. B **59**, R10417 (1999).
[33] A.V. Sologubenko *et al.* Phys. Rev. B **66**, 014504 (2002).